OCCAM

OXFORD CENTRE FOR COLLABORATIVE APPLIED MATHEMATICS

On the anomalous dynamics of capillary rise in porous media

by

Yulii D. Shikhmurzaev
James E. Sprittles

OCCAM Preprint Number 12/56

On the anomalous dynamics of capillary rise in porous media

Yulii D. Shikhmurzaev*
School of Mathematics, University of Birmingham, Birmingham, B15 2TT, UK.

James E. Sprittles†
Mathematical Institute, University of Oxford, Oxford OX1 3LB, UK.

(Dated: June 19, 2012)

The anomalous dynamics of capillary rise in a porous medium discovered experimentally more than a decade ago (Delker et al., Phys. Rev. Lett. 76 (1996) 2902) is described. The developed theory is based on considering the principal modes of motion of the menisci that collectively form the wetting front on the Darcy scale. These modes, which include (i) dynamic wetting mode, (ii) threshold mode and (iii) interface de-pinning process, are incorporated into the boundary conditions for the bulk equations formulated in the regular framework of continuum mechanics of porous media, thus allowing one to consider a general case of three-dimensional flows. The developed theory makes it possible to describe all regimes observed in the experiment, with the time spanning more than four orders of magnitude, and highlights the dominant physical mechanisms at different stages of the process.

PACS numbers: 47.56.+r, 68.03.Cd, 68.05.-n

I. INTRODUCTION

The propagation of the liquid-fluid interfaces through porous media is central to a wide range of natural phenomena and industrial applications, with the latter including enhanced oil recovery, hydrogeology, fuel cells, carbon dioxide sequestration to mention but a few. This topic remains the subject of intensive research, both experimental and theoretical, comprehensively reviewed in a number of articles over the past forty years [1–5]. The main aspects of research have been the rate of propagation of the wetting front [6–9], the wetting front's roughening [10, 11] and stability [12], as well as the related problems of the formation and dynamics of the pockets of the displaced phase (bubbles, ganglia) left behind the front [2, 13, 14]. The first of these aspects is of particular importance as it ultimately determines the main macroscopic characteristics of the process in many applications.

As has been discovered experimentally more than a decade ago by Delker and his co-workers [15], besides the common situation where a wetting front propagates through a porous medium broadly in accordance with Washburn's model [16], which balances the driving force due to the (presumed constant) capillary pressure of a meniscus and viscous resistance as in the Poiseuille-type flow, for some media, such as porous matrices made of packed spherical beads, the initial Washburn-type imbibition is followed by a completely different and in many ways 'anomalous' regime. A representative set of data taken from [15] is shown in Fig. 1. Similar results have been reported later by Lago and Araujo [17]. The essence of the discovered effect is that, if the height h of the capillary rise (measured from some initial level to remove from consideration the entrance effects) is plotted against time t on the log-log scale (Fig. 1), one can immediately see two distinct regions. Roughly speaking, for about two minutes the liquid climbs 2/3 of its eventual (maximum) height h_{max} in the Washburn-like regime after which it takes many hours for it to advances across the remaining 1/3 of h_{max}, with the wetting front moving in small-amplitude jumps on the pore scale [17]. The log-log plot of this second regime shows a clear concave-convex sequence which indicates that the dynamics there is more complex than what one would expect from some power-law fit and the accompanying arguments. Another intriguing feature of the phenomenon is that h_{max} is determined by the balance of capillarity and gravity, i.e. the factors that, together with viscous resistance, determine the dynamics of the Washburn regime, although what looked like the Washburn regime has been abandoned after a couple of minutes from the onset of the capillary rise and for hours the process is distinctly non-Washburnian.

The experimental data has been discussed qualitatively in terms of interface pinning and random capillary forces [15, 17], but on the quantitative level the only outcome is that a simple equation

$$dh/dt = v_0(F/F_T - 1)^\beta \tag{1}$$

expressing the rate of the capillary rise as a function of a driving force F and a threshold value F_T leads to an "anomalously large" exponent β [15], so that h deviates from the experimental data for small times and unphysically diverges as time goes to infinity. The dashed line in Fig. 1 corresponds to

$$h = H_c - (H_c - h_1)[1 + A(t - t_1)]^{1/(1-\beta)} \tag{2}$$

that has been deduced from (1) and used in [15]; the values of the constants H_c, h_1, A, t_1 and β are given in [15]. Although the fitting curve (2) is able to describe only a

* Y.D.Shikhmurzaev@bham.ac.uk
† sprittles@maths.ox.ac.uk

finite time span, the general ideas of the interface pinning and random forces that might de-pin the interface and allow it to move further seem fruitful, and a question that arises naturally is how to embed them into the regular framework of continuum mechanics of porous media, as opposed to just using *ad hoc* semi-empirical equations for the wetting front evolution in a one-dimensional flow. Below, we address this question on the basis of an earlier developed approach to the modelling of the wetting front dynamics in porous media based on considering different modes of motion that menisci go through on the pore scale and the corresponding technique of conjugate problems [18]. Then, we will discuss how the experimental phenomenon in question is seen through other modelling approaches.

II. MACROSCOPIC (DARCY-SCALE) DESCRIPTION

In the continuum framework, the wetting front $\partial\Omega_1$ is a moving boundary which, together with other boundaries $\partial\Omega_2$, confines a domain Ω where the Darcy equation,

$$\mathbf{u} = -(\kappa/\mu)\nabla(p + \rho g z), \qquad (\mathbf{r} \in \Omega), \tag{3}$$

and the continuity equation, $\nabla\cdot\mathbf{u} = 0$, for the average velocity $\mathbf{u}$ and pressure p operate. Then, the wetting front evolution is part of the solution of a properly formulated problem for these bulk equations. The Darcy equation (3) is written in the form already accounting for gravity with ρ being the density of the liquid, g the gravitational acceleration, z the coordinate directed against gravity, κ the permeability of the porous matrix and μ the liquid's viscosity; the coordinates are represented in terms of the position vector $\mathbf{r}$; hereafter the pressure is measured with respect to the (presumed constant) pressure in the displaced gas.

An appropriate starting point for the modelling is the recently developed approach [18] that gives boundary conditions for Laplace's equation for p,

$$\nabla^2 p = 0, \qquad (\mathbf{r} \in \Omega), \tag{4}$$

which follows from the Darcy and continuity equations above and can be used to replace the latter. The key idea of this approach is to consider the *modes of motion* which the menisci that collectively form the wetting front undergo as the wetting front propagates. The simplest model formulated in the framework of this approach accounts for the two main modes: (i) the wetting mode, where, on the pore scale, the contact line moves forward, essentially in the Washburn regime but accounting for a *dynamic*, i.e. velocity-dependent, contact angle θ_d, and (ii) the threshold mode, where the contact line gets pinned and the meniscus bends as the pressure on it increases until the contact angle reaches some threshold value θ_* when the meniscus can go back into the wetting mode with the contact line moving again. This

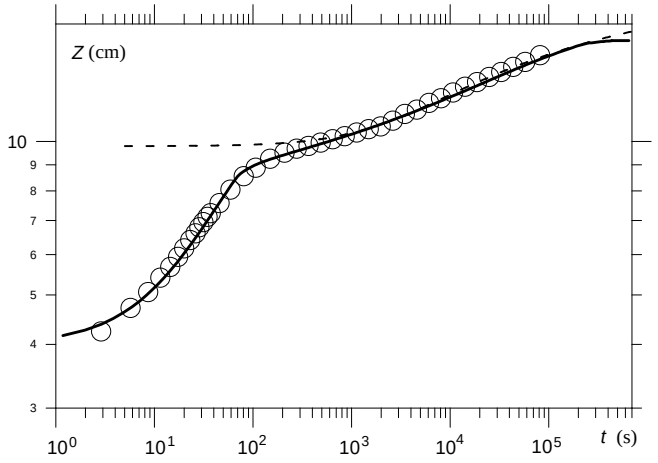

FIG. 1. Time-dependence of the imbibition height in 1D capillary rise. Circles: experimental data from [15] for beads 253 μm in diameter; dashed line: fit considered in [15]; solid line: present theory.

increase of pressure on the meniscus as the contact line gets pinned is similar to what one would have on a piston sucking a liquid into a pipe if the motion of the piston is blocked. For the porous medium, the maximum possible pressure on the meniscus in the threshold mode, $\bar{p}|_{\partial\Omega_1}$, is the solution of a *conjugate* problem [18]

$$\nabla^2\bar{p} = 0, \quad (\mathbf{r} \in \Omega); \qquad \mathbf{n}\cdot\nabla(\bar{p} + \rho g z)|_{\partial\Omega_1} = 0, \tag{5}$$

with the boundary condition for $\bar{p}$ on $\partial\Omega_2$ being the same as for p; $\mathbf{n}$ is the outward normal to $\partial\Omega_1$. Thus, the idea of the interface pinning is already in the model, used in formulating the boundary conditions on the wetting front that we will recapitulate below, and in this work we consider how the model can be generalized to incorporate the idea of random forces that could lead to de-pinning of the interface and describe the observed features of the phenomenon mentioned earlier.

On the moving wetting front the kinematic and dynamic boundary conditions for (4) have the form

$$\frac{\partial f}{\partial t} + \mathbf{u}\cdot\nabla f = 0, \tag{6}$$

$$p = A_1 p_1 + A_2 p_2, \quad (\mathbf{r} \in \partial\Omega_1), \tag{7}$$

where for a one-dimensional capillary rise $f(\mathbf{r}, t) \equiv z - h(t)$, p_1, p_2 are the averaged pressures and A_1, A_2 are the spatio-temporally averaged fractions of the unit area of the free surface corresponding to the two modes of motion ($A_1 + A_2 = 1$). For the wetting mode one has

$$p_1 = -2\sigma\cos\theta_d/a, \tag{8}$$

where σ is the liquid-gas surface tension, a is the effective radius of the capillary and the dependence of the dynamic contact angle θ_d on the meniscus speed u_1 is given by

[18, 19]

$$\frac{u_1}{U_{cl}} = \left(\frac{(1 + (1 - \rho^s_{1e}) \cos\theta_s)(\cos\theta_s - \cos\theta_d)^2}{4(\cos\theta_s + B)(\cos\theta_d + B)} \right)^{1/2}, \tag{9}$$

where $B = (1 - \rho^s_{1e})^{-1}(1 + \rho^s_{1e} u_0(\theta_d))$, θ_s is the static contact angle,

$$u_0(\theta_d) = \frac{\sin\theta_d - \theta_d \cos\theta_d}{\sin\theta_d \cos\theta_d - \theta_d}, \qquad U_{cl} = \left(\frac{\gamma \rho^s_0 (1 + 4\alpha\beta)}{\tau\beta} \right)^{1/2}$$

is the characteristic speed associated with the parameters that the 'additional' physics of wetting brings in to resolve the well-known 'moving contact-line problem' [19–21], ρ^s_0, ρ^s_{1e}, α, β, γ, τ are material constants characterizing the contacting media whose values can be found elsewhere [19, 22].

In the threshold mode, the contact line gets pinned and the meniscus, experiencing an increase in pressure on it, bends so that the contact angle varies from θ_d, i.e. the value with which the meniscus arrives at the threshold mode, to θ_*, which is the value at which the meniscus 'breaks through' the threshold and the process goes back to the wetting mode. From the dynamics of this type of motion, under the assumption that the meniscus retains the shape of a spherical cap with its radius varying as the meniscus bends, one has that [18]

$$u_2 = aJ(\theta_d)T^{-1}, \tag{10}$$

$$p_2 = P - \frac{2\sigma}{u_1 T} \left(\frac{Pa}{2\sigma} + \cos\theta_d \right) J(\theta_d), \tag{11}$$

where

$$P = \bar{p}|_{\partial\Omega_1}, \tag{12}$$

$$J(\theta_d) = \left[\frac{1}{2} \tan\left(\frac{\theta}{2} - \frac{\pi}{4} \right) + \frac{1}{6} \tan^3\left(\frac{\theta}{2} - \frac{\pi}{4} \right) \right]_{\theta_d}^{\theta_*},$$

$[f]_a^b \equiv f(b) - f(a)$, and the time T that the meniscus spends in the threshold mode is given by

$$T = T_2\left(\theta_d, \frac{Pa}{2\sigma}\right) \equiv a u_1^{-1} \left(\frac{Pa}{2\sigma} + \cos\theta_d \right) I\left(\theta_d, \frac{Pa}{2\sigma}\right), \tag{13}$$

$$I\left(\theta_d, \frac{Pa}{2\sigma}\right) = \int_{\theta_d}^{\theta_*} \frac{d\theta}{(1 + \sin\theta)^2 (Pa/(2\sigma) + \cos\theta)}.$$

For a one-dimensional capillary rise, as follows from (5), the stagnation pressure $\bar{p}|_{\partial\Omega_1}$ is given simply by $\bar{p}|_{\partial\Omega_1} = p_0 - \rho g h(t)$, where p_0 is the prescribed pressure at $z = 0$.

Finally, the velocity of the wetting front as a whole, $u_n = \mathbf{n} \cdot \mathbf{u}|_{\partial\Omega_1}$ is given by an expression

$$u_n = A_1 u_1 + A_2 u_2, \tag{14}$$

which is similar to (7). For the menisci intermittently going through the wetting and threshold modes as the wetting front propagates, the coefficients A_1 and A_2 can be viewed as reflecting the fraction of the time spent in each mode as the meniscus travels over the length of averaging that introduces the Darcy scale (or, equivalently, the fraction of the interfacial area corresponding to each mode of motion over the time interval of averaging that introduces the Darcy time scale), i.e. the spatio-temporal averages we mentioned earlier. They are given by [18]

$$A_1 = \frac{s_1 u_2}{s_2 u_1 + s_1 u_2}, \quad A_2 = \frac{s_2 u_1}{s_2 u_1 + s_1 u_2}, \tag{15}$$

where

$$s_1(\theta_d, \theta_*) = \begin{cases} 1, & \theta_d - \theta_* \geq 0 \\ s_{10}, & \theta_d - \theta_* < 0 \end{cases}, \qquad s_2 = 1 - s_1, \tag{16}$$

and s_{10} (< 1) is a characteristic of the porous matrix. Then, as should be expected, the slowest (controlling) mode of motion makes a greater contribution to the average pressure and velocity at the wetting front, and if the velocity u_i corresponding to the ith mode reaches zero, one will have $A_i = 1$ and the pressure at the wetting front, that is now at rest, will become equal to p_i. Thus, the wetting front will stop propagating in two cases: (a) $u_1 = 0$ and hence $\theta_d = \theta_s$, which means that the meniscus has reached its equilibrium state corresponding to the maximum imbibition height h_{max}, and (b) $u_2 = 0$ so that the wetting front still has a capacity to propagate further but the contact line became pinned (threshold mode) and the pressure that mounts on the meniscus in this case, even when it reaches its maximum possible value $\bar{p}|_{\partial\Omega_1}$, is insufficient to push the meniscus through. Mathematically, in the last case we have that $\bar{p}|_{\partial\Omega_1}$, which goes down as h increases, becomes equal to $p_* = -2\sigma\cos\theta_*/a$ and hence is unable to make the contact angle greater than θ_*, which would allow the meniscus to resume its motion in the wetting mode: in this case $I(\theta_d, Pa/(2\sigma))$ and hence the time T go to infinity. The height corresponding to this last case depends only on θ_*, and the meniscus reaches it in a finite time [18].

III. SUBCRITICAL INTERFACE DE-PINNING

It is convenient to introduce the 'stagnation' contact angle $\bar{\theta}$ corresponding to the stagnation pressure $\bar{p}|_{\partial\Omega_1}$ by $\bar{\theta} = \arccos(-\bar{p}|_{\partial\Omega_1} a/(2\sigma))$. Then, if $\bar{\theta} > \theta_s$, the wetting front has the potential to propagate but if at the same time $\bar{\theta} \leq \theta_*$ the stagnation pressure $\bar{p}|_{\partial\Omega_1}$ is unable to push the meniscus through the threshold mode. In a sense, $\theta_* - \bar{\theta}$ can be viewed as a quantitative measure of the potential barrier that has to be overcome to get the meniscus back into the wetting mode when $\bar{p}|_{\partial\Omega_1}$ is 'subcritical', i.e. less than p_*, and hence unable to push the meniscus through the threshold.

Importantly, since, until the wetting front reaches its equilibrium position at the maximum height, at every

moment individual menisci are not in the same mode of motion (and, for the threshold motion, not even in the same stage of it), the Darcy-scale pressures we are considering, including the stagnation pressure $\bar{p}|_{\partial\Omega_1}$, represent average values, whereas on the pore scale one also has pressure fluctuations due to mutual influences of menisci. These fluctuations are unimportant when the stagnation pressure $\bar{p}|_{\partial\Omega_1}$ is capable of pushing the meniscus through the threshold mode. However, as $\bar{p}|_{\partial\Omega_1}$ goes down to p_*, the time T needed to overcome the threshold increases, so that, when it becomes large enough, it is the fluctuations that increasingly become the mechanism of de-pinning, and when $\bar{\theta} \le \theta_*$ it is only the random fluctuations that can de-pin the menisci.

The simplest way of accounting for the subcritical de-pinning due to random fluctuations as this mechanism takes over from the 'regular' de-pinning due to the stagnation pressure is to assume that, once T_2 becomes greater than a certain value T_+, it is these random factors that will de-pin the interface and determine the time it stays in the threshold mode. For the 'regular' stagnation pressure $\bar{p}|_{\partial\Omega_1}$ one has that $T_2 \to \infty$ as $\bar{p}|_{\partial\Omega_1} \to p_*$ and $\bar{p}|_{\partial\Omega_1}$ is no longer able to push the meniscus through when $\bar{p}|_{\partial\Omega_1} < p_*$. The probability of the random factors de-pinning the interface should be expected to go down as $p_* - \bar{p}|_{\partial\Omega_1}$ (or equivalently $\theta_* - \bar{\theta}$) increases. The simplest way of generalizing the model to incorporate the above scenario mathematically is to replace (13) and (12) respectively with

$$T = \begin{cases} T_2\left(\theta_d, \dfrac{a\bar{p}|_{\partial\Omega_1}}{2\sigma}\right), & \text{if } T_2(\bar{p}|_{\partial\Omega_1}) \le T_+ \\ T_+ + k(\theta_+ - \bar{\theta})^2, & \text{if } T_2(\bar{p}|_{\partial\Omega_1}) > T_+ \end{cases}, \qquad (17)$$

$$P = \begin{cases} \bar{p}|_{\partial\Omega_1}, & \text{if } T_2(\bar{p}|_{\partial\Omega_1}) \le T_+ \\ p_+, & \text{if } T_2(\bar{p}|_{\partial\Omega_1}) > T_+ \end{cases}, \qquad (18)$$

where p_+ is determined by $T_2(p_+) = T_+$, and $\theta_+ = \arccos(-p_+ a/(2\sigma))$. Since T_2 rises steeply only when $\bar{\theta}$ is close to θ_*, in practice one has that $\theta_+ \approx \theta_*$ and $p_+ \approx p_*$.

Now, we have a closed model, which, unlike *ad hoc* formulae for one-dimensional propagation of the wetting front, is applicable for a general case of three-dimensional flows. In order to describe a particular flow involving a moving wetting front, one has to solve Laplace's equation (4) for p in Ω whose boundary $\partial\Omega_1$ evolves according to (6), where $\mathbf{u}$ is given by (3), subject to the dynamic condition (7), where equations (8)–(11), (14)–(18) close the formulation and $\bar{p}|_{\partial\Omega_1}$ is the solution of the conjugate problem (5); the boundary conditions on $\partial\Omega_2$ for both p and $\bar{p}$ are the same and, together with the initial shape of Ω, they specify a particular problem.

In the case of a one-dimensional capillary rise Laplace's equations for p and $\bar{p}$ give that these are linear functions of z, and equations (3), (4), (6) yield

$$\frac{dh}{dt} = \frac{\kappa}{\mu}\left(\frac{p_0 - p(h,t)}{h} - \rho g\right),$$

which together with the algebraic equations (7), where $p|_{\partial\Omega_1} \equiv p(h,t)$, (8)–(11), (14), where $u_n = dh/dt$, (15)–(18), with $\bar{p}|_{\partial\Omega_1} = p_0 - \rho g h$ as the solution of the conjugate problem, form a closed system for h, $p(h,t)$, p_1, θ_d, u_1, u_2, p_2, A_1, A_2, s_1 and s_2. The results of comparing the numerical solution corresponding to the experimental flow conditions of [15] with the data are shown in Fig. 1. As one can see, the solid curve representing the computed solution describes the data very well over the whole time period spanning more than four orders of magnitude. The theoretical curve also levels off as $t \to \infty$, indicating that the capillary rise does eventually come to a halt. Comparison of the theory with all four sets of experimental data from [15] is shown in Fig. 2. (The dashed line in this figure is used to indicate that for the beads' diameter of 510 μm, strictly speaking, the theory is used outside its limits of applicability as the whole advancement of the wetting front is less than 40 beads' diameters, so that it is difficult to talk about the separation of scales required for the continuum mechanics approach to work. Indeed, for this approach to be applicable, there should exist an intermediate scale much larger than the pore size and at the same time much smaller than the macroscopic length scale on which the flow is described. In the case of 510 μm beads, 'much large' and 'much smaller' would mean 6 times larger or smaller, which is clearly not sufficient to ensure acceptable accuracy.)

It is noteworthy that, although the initial regime where the curve in Fig. 1 rises steeply looks Washburn-like, it actually involves both the wetting and the threshold modes of motion. As in [18], the presence of the threshold-overcoming motion becomes pronounced only when h climbs close to $h_* = (p_0 - p_*)/(\rho g)$, i.e. when $\bar{p}$ becomes close to p_* or, in other words, $\bar{\theta}$ close to θ_*. For the results presented in Fig. 1 $\theta_* = 67°$, $\theta_s = 0°$, $s_{10} = 0.7$, $\mu U_{cl}/(\kappa\rho g) = 10^2$, $\rho^s_{1e} = 0.6$, $T_+/T_0 = 3$, $k/T_0 = 4 \times 10^3$, where $T_0 = 2\sigma\mu/((\rho g)^2 a\kappa)$, and it is θ_s, θ_*, T_+/T_0 and k/T_0 that are most important. Since in the experiment, as described in [15], the bottom of the test section was located approximately 4 cm above the bottom of the porous sample, we have to start the calculations from the bottom of the sample with $p_0 = \rho g Z_{ini}$, $Z_{ini} = 4$ cm and, to compare theory with the data, measure the time from the moment the wetting front reaches Z_{ini}. To describe the data in Fig. 2, only a variation of θ_* and $K = k/T_0$ is required: $\theta_{*180} = 64°$, $\theta_{*253} = 67°$, $\theta_{*359} = 78°$; $K_{359} = 3K_{253} = 12K_{180}$., $K_{180} = 10^3$.

It is worth mentioning that, although in the model we represent capillary effects in the pores using the capillary pressure and viscous resistance corresponding to an 'effective' circular cross-section, whereas in the experiment with the porous matrix made of spherical beads neither the 'chambers' nor the 'throats' of the porous medium had circular cross-sections, no adjustment of the results was required: we used the radius of the bead as a in the model with no subsequent calibration of the time and length scales. This shows that a 'representative' way

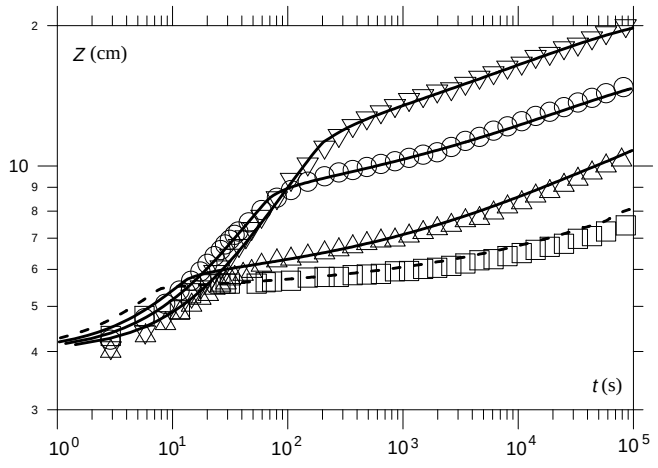

FIG. 2. All four experimental sets from [15] for beads' diameters 180 μm ($\triangledown$), 253 μm ($\circ$), 359 μm ($\triangle$), and 510 μm ($\square$). The corresponding theoretical curves are given as solid lines for the first 3 sets of data and as a dashed line for the last.

of modelling the porous medium, as opposed to much more difficult way of incorporating into a model the exact porous structure determined via elaborate and expensive experiments, allows one to incorporate all the main features of the process on the pore scale, including the actual physics of dynamic wetting, and obtain good results for the flow on the Darcy scale.

IV. DISCUSSION

It is instructive to look at the obtained theoretical result and the experiment it addresses from the viewpoint of the different modelling approaches used to describe two-phase flows in porous media. These approaches broadly fall into two general classes, 'representative' and 'simulative'. They are not antagonistic as, in theory, if the same pore-scale physics and the same characteristics of the porous medium are accounted for in the models formulated in the framework of each of these approaches, then the results produced by these models are expected to converge and describe the same macroscopic behaviour of the wetting front.

The present model has been developed in the framework of the 'representative' approach, where the equations and boundary conditions are formulated on the Darcy scale, i.e. the scale implying that the continuum limit has already been taken, and the properties of the porous matrix are 'represented' in terms of the permeability coefficient (or tensor, if the porous medium is anisotropic), effective size of the pores (or the corresponding distribution), effective threshold angles, etc. Importantly, since the pore-scale wetting process is modelled realistically, with the velocity (as well as material) dependence of the dynamic contact angle, the model captures naturally that the wetting front has the capacity to move forward when the contact angle is greater than the static value θ_s, i.e. when the interface has not reached its maximum height determined by the balance of capillary and gravity forces. In other words, as the meniscus gets de-pinned, the fact that the contact angle differs from its equilibrium value θ_s and that the dynamic contact angle is velocity-dependent act as a mechanism that moves the interface until the dynamic contact angle goes down to θ_s and the interface reaches its maximum height.

The subcritical de-pinning mechanism that comes into action when $\bar{p}|_{\partial\Omega_1} \leq p_*$ is formulated implicitly, in terms of the 'potential barrier' $\theta_+ - \bar{\theta}$ and the 'waiting time' $T_+ + k(\theta_+ - \bar{\theta})^2$ required for the random fluctuations to overcome it. Both of these characteristics are Darcy-scale parameters. A natural way to develop the model further would be to remove the direct link between the 'potential barrier' and the 'waiting time' and instead explicitly introduce the field of pressure fluctuations depending on the flow rate and properties of the porous matrix. Then, this pressure fluctuation field becomes an addition to $\bar{p}|_{\partial\Omega_1}$ as a breakthrough factor. For this explicitly introduced mechanism, the results obtained in the present work would serve as a guideline, indicating one of the outcomes that this mechanism should produce.

The implicit mechanism of the subcritical interface depinning on the Darcy scale that we have introduced can be viewed as a macroscopic manifestation of the dynamics of avalanches [23]. Avalanches qualitatively stem from the same physics as the one considered here and, in a sense, can be regarded as a medium-scale phenomenon, i.e. between the pore scale and the Darcy scale. The idea of linking the Darcy-scale subcritical interface depinning and the dynamics of avalanches agrees with the fact that the avalanche-type events have been observed experimentally by Lago and Araujo [17] in the anomalous regime of the wetting front propagation. The avalanche behaviour of the wetting fronts is currently being investigated in terms of scaling laws [24], and the present theory, with its explicit accounting for different pressures corresponding to different modes of motion and their spatio-temporal weights, offers a macroscopic framework for the mathematical description of these medium-scale events. Then, the subcritical interface de-pinning in the anomalous regime of the wetting front propagation could be viewed as the macroscopic outcome of a succession of avalanches with decreasing probabilities.

The 'simulative' approach to the modelling of two-phase flows in porous media is based on replacing the actual porous matrix with a regular network of 'chambers' and capillary 'throats' connecting them [25–29]. In order to partially compensate the anisotropy inherent in this approach where, as is the case in most works, the chambers are placed at the nodes of a regular lattice, the sizes of both chambers and throats are made random following certain prescribed distributions. The macroscopic (Darcy-scale) characteristics of the process are obtained as a result of the appropriate averaging. The simulative approach has the appeal of what looks like a numerical experiment offering a transparent link between the

pore-scale and the Darcy-scale dynamics, but, unlike the case of molecular-dynamics simulations with regard to macroscopic fluid mechanics, this appeal is moderated by a number of factors, notably the fact that the actual dynamics on the pore scale is not computed. Instead, it is essentially represented in terms of a Washburn-type dynamics, thus by-passing the 'moving contact-line problem' [20] and the associated physics of dynamic wetting [21, 30]. It is also important to note that the rigid geometric structure of the network simulating the actual porous matrix imposes unavoidable limitations on the macroscopic transport properties of the porous medium that the network is purports to simulate. By contrast, the representative approach can introduce any tensorial and topological characteristics of the porous medium that the corresponding model requires. Having in mind the above shortcomings of the representative approach, it is interesting to look at what it can produce with regard to the anomalous regime of the wetting front propagation.

Bijeljic *et al.* [29] performed the network modelling of the capillary rise and compared their results to the truncated set of data taken from Lago and Araujo [17], with the original experiment by Delker et al. [15] mentioned but not used for comparison with the simulations. The simulations agree well with the experimental data for the times $t \leq 4\times10^4$ s after which the simulated height levels off. However, when one takes the full set of experimental data reported by Lago and Araujo, i.e. for the times up to $t = 2 \times 10^5$ s, one can immediately see that the wetting front continues to climb. It is also worth noting that the simulated height-vs-time curve in the log-log coordinates is convex, with the slope monotonically decreasing, whereas, as one can see in Fig. 1, the experimental data show a distinct concave-convex sequence, i.e. after an initial decrease as the anomalous regime is entered the slope picks up again until, finally, the data start to level off, asymptotically approaching the maximum height. The same trend was observed earlier by Diggins *et al.* [31] whose data are given in Fig. 12 of Lago and Araujo [17]. This figure in [17] also clearly shows that, although the time-dependence of the height of the capillary rise following from the Washburn-type interplay of capillarity, viscosity and gravity can describe the 'regular' regime *and* be fitted to the initial stage of the 'anomalous' regime, it is nowhere near a satisfactory description of the latter once the full set of data is considered, as the height-vs-time curve in the logarithmic coordinates picks up again and climbs much higher than the above fitting predicts.

From the viewpoint of the theory developed in the present work, the main deficiency of the currently implemented network models is that they essentially deal only with one — wetting — mode of motion of the menisci. Then, setting aside the minor (in comparison with the effects considered here) variations introduced by randomizing the size distributions, these models broadly reproduce the Washburn-type dynamics of the wetting front. As a result, once gravity starts to balance capillarity as the driving force, the wetting front slows down and comes to a halt. Essentially, the fitting of the simulated curve to the experimental data for the very beginning of the anomalous regime is produced by adjusting the maximum height of the capillary rise, whereas, as we pointed out in the introduction, the intriguing feature of the anomalous regime is precisely the fact that it lies in between the 'normal' Washburnian regime of the imbibition and the maximum height that is also Washburnian.

The capillary network approach can be modified in a relatively straightforward way to account for the threshold mode of motion. The main element in this modification should be equipping the 'chambers' with threshold characteristics, such as the pressure required to overcome the threshold, which, besides material properties, can depend on the number of menisci reaching the same chamber. The implementation of the subcritical de-pinning is more challenging as this would require accounting for fluctuations of pressure experienced by the liquid, i.e. replacing the Washburn-type models of the flow in the 'throats' by an essentially unsteady motion that takes into account the unsteady processes in the neighboring chambers and throats. An intermediate check for such a model could be its ability to produce avalanches as the medium-scale phenomena that on the Darcy scale result in the anomalous regime of imbibition.

V. CONCLUSION

The developed theory shows that the new approach to the modelling of the propagation of wetting fronts in porous media based on considering specific modes of motion that the menisci of the pore scale undergo as the front propagates allows one to incorporate critical phenomena and adequately describe experimental data for the anomalous regime of imbibition. Accounting for the random pore-scale forces macroscopically, in terms of the 'potential barriers' and the corresponding times required for the random forces to overcome these barriers, allowed the simplest model formulated in the framework of the new approach to describe the whole experimental curve, from the Washburn regime to the (also Washburn) maximum imbibition height with the anomalous regime in between. The proposed theory could be used as a guide for the porous network modelling and the study of the anomalous imbibition regime as the manifestation of the dynamics of avalanches.

This publication was based on work supported in part by Award No. KUK-C1-013-04 , made by King Abdullah University of Science and Technology (KAUST).

[1] R. A. Wooding and H. J. Morel-Seytoux, Annu. Rev. Fluid Mech. **8**, 233 (1976).
[2] A. C. Payatakes, Annu. Rev. Fluid Mech. **14**, 365 (1982).
[3] P. M. Adler and H. Brenner, Annu. Rev. Fluid Mech. **20**, 35 (1988).
[4] W. L. Olbricht, Annu. Rev. Fluid Mech. **28**, 187 (1996).
[5] M. Alava, M. Dubé, and M. Rost, Adv. Phys. **53**, 83 (2004).
[6] L. Labajos-Broncano, M. I. González-Martin, J. M. Bruque, C. M. González-García, and B. Jańczuk, J. Colloid Interf. Sci. **219**, 275 (1999).
[7] J. Schoelkopf, C. J. Ridgway, P. A. C. Gane, P. Matthews, and D. C. Spielmann, J. Colloid Interf. Sci. **227**, 119 (2000).
[8] M. Gombia, V. Bortolotti, R. J. S. Brown, M. Camaiti, and P. Fantazzini, J. Appl. Phys. **103**, 094913 (2008).
[9] M. Reyssat, L. Y. Sangne, E. A. van Nierop, and H. A. Stone, Europhys. Lett. **86**, 56002 (2009).
[10] V. K. Horváth and H. E. Stanley, Phys. Rev. E **52**, 5166 (1995).
[11] J. Soriano, A. Mercier, R. Planet, A. Hernández-Machado, M. A. Rodríguez, and J. Ortín, Phys. Rev. Lett. **95**, 104501 (2005).
[12] B. P. Tullis and S. J. Wright, Transp. Porous Media **70**, 335 (2007).
[13] M. G. Bernadiner, Transp. Porous Media **30**, 251 (1998).
[14] T. Suekane, N. Zhou, T. Hosokawa, and T. Matsumoto, Transp. Porous Media **82**, 111 (2010).
[15] T. Delker, D. B. Pengra, and P.-z. Wong, Phys. Rev. Lett. **76**, 2902 (1996).
[16] E. W. Washburn, Phys. Rev. **17**, 273 (1921).
[17] M. Lago and M. Araujo, J. Colloid Interf. Sci. **234**, 35 (2001).
[18] Y. D. Shikhmurzaev and J. E. Sprittles, J. Fluid Mech. **694**, 399 (2012).
[19] Y. D. Shikhmurzaev, *Capillary Flows with Forming Interfaces* (Chapman & Hall/CRC, Boca Raton-London-New York, 2007).
[20] E. B. Dussan V., Annu. Rev. Fluid Mech **11**, 371 (1979).
[21] Y. D. Shikhmurzaev, Euro. Phys. J. - Special Topics **197**, 47 (2011).
[22] T. D. Blake and Y. D. Shikhmurzaev, J. Colloid Interf. Sci. **253**, 196 (2002).
[23] A. Dougherty and N. Carle, Phys. Rev. E **58**, 2889 (1998).
[24] M. Rost, L. Laurson, M. Dube, and M. Alava, Phys. Rev. Lett. **98**, 054502 (2007).
[25] I. Fatt, Trans. ASME **207**, 164 (1956).
[26] R. Lenormand, E. Touboul, and C. Zarcone, J. Fluid Mech. **189**, 165 (1988).
[27] E. Aker and K. J. Måløy, Phys. Rev. E **61**, 2936 (2000).
[28] V. Joekar-Niasar, S. M. Hassanizadeh, and H. K. Dahle, J. Fluid Mech. **655**, 38 (2010).
[29] B. Bijeljic, B. Markicevic, and H. K. Navaz, Phys. Rev. E **83**, 056310 (2011).
[30] T. D. Blake, J. Colloid & Interf. Sci. **299**, 1 (2006).
[31] D. Diggins, L. G. J. Fokkink, and J. Ralston, Colloids & Surf. **44**, 299 (1990).

RECENT REPORTS

12/33	Second weak order explicit stabilized methods for stiff stochastic differential equations	Abdulle Vilmart Zygalakis
12/34	The sensitivity of Graphene 'Snap-through' to substrate geometry	Wagner Vella
12/35	The physics of frost heave and ice-lens growth	Peppin Style
12/36	Finite Element Simulation of Dynamic Wetting Flows as an Interface Formation Process	Sprittles Shikhmurzaev
12/37	The Dynamics of Liquid Drops and their Interaction with Solids of Varying Wettabilities	Sprittles Shikhmurzaev
12/38	Dispersal and noise: Various modes of synchrony in ecological oscillators	Bressloff Lai
12/39	Boundary conditions for free surface inlet and outlet problems	Taroni Breward Howell Oliver
12/40	A Branch and Bound Algorithm for the Global Optimization of Hessian Lipschitz Continuous Functions	Fowkes Gould Farmer
12/41	The Orthogonal Gradients Method: a Radial Basis Functions Method for Solving Partial Differential Equations on Arbitrary Surfaces	Piret
12/42	Squeeze-Film Flow in the Presence of a Thin Porous Bed, with Application to the Human Knee Joint	Knox Wilson Duffy McKee
12/43	Gravity-driven draining of a thin rivulet with constant width down a slowly varying substrate	Paterson Wilson Duffy
12/44	The 'Sticky Elastica': Delamination blisters beyond small deformations	Wagner Vella
12/45	Stochastic models of intracellular transport	Bressloff Newby
12/46	The effects of noise on binocular rivalry waves: a stochastic neural field model	Webber Bressloff

12/47	An Ensemble Bayesian Filter for State Estimation	Farmer
12/48	Simulation of cell movement through evolving environment: a fictitious domain approach	Séguis Burrage Erban Kay
12/49	The Mathematics of Liquid Crystals: Analysis, Computation and Applications	Majumdar
12/50	Fourier spectral methods for fractional-in-space reaction-diffusion equations	Bueno-Orovio Kay Burrage
12/51	Meniscal tear film fluid dynamics near Marx's line	Zubkov Breward Gaffney
12/52	Validity of the Cauchy-Born rule applied to discrete cellular-scale models of biological tissues	Davit Osborne Byrne Gavaghan Pitt-Francis
12/53	A thin rivulet or ridge subject to a uniform transverse shear stress at its free surface due to an external airflow	Sullivan Paterson Wilson Duffy
12/54	The Stokes boundary layer for a thixotropic or antithixotropic fluid	McArdle Pritchard Wilson
12/55	Thermoviscous Coating and Rimming Flow	Leslie Wilson Duffy

Copies of these, and any other OCCAM reports can be obtained from:

Oxford Centre for Collaborative Applied Mathematics
Mathematical Institute
24 - 29 St Giles'
Oxford
OX1 3LB
England
www.maths.ox.ac.uk/occam